Synthesis and Evaluation of Heteroaryl-Substituted Dihydronaphthalenes and Indenes: Potent and Selective Inhibitors of Aldosterone Synthase (CYP11B2) for the Treatment of Congestive Heart Failure and Myocardial Fibrosis

Marieke Voets,[†] Iris Antes,[‡] Christiane Scherer,[†] Ursula Müller-Vieira,[†] Klaus Biemel,[§] Sandrine Marchais-Oberwinkler,[†] and Rolf W. Hartmann*,[†]

8.2 Pharmaceutical and Medicinal Chemistry, Saarland University, P.O. Box 15 11 50, D-66041 Saarbruecken, Germany, Max Planck Institute for Informatics, Stuhlsatzenhausweg 85, D-66123 Saarbruecken, Germany, and Pharmacelsus CRO, Science Park 2, D-66123 Saarbruecken, Germany

Received January 17, 2006

In this study, the synthesis and biological evaluation of heteroaryl-substituted dihydronaphthalenes and indenes (**1**−**16**) is described. The compounds were tested for activity by use of human CYP11B2 expressed in fission yeast and V79 MZh cells and for selectivity by use of human CYP11B1, CYP17, and CYP19. The most active inhibitor was the 6-methoxydihydronaphthalene **4** (IC_{50} = 2 nM), showing a K_i value of 1.3 nM and a competitive type of inhibition. The 5-methoxyindene **3** was found to be the most selective CYP11B2 inhibitor (IC_{50} = 4 nM; CYP11B1 IC_{50} = 5684 nM), which also showed only marginal inhibition of human CYP3A4 and CYP2D6. Docking and molecular dynamics studies using our homology-modeled CYP11B2 structure were performed to understand some structure−activity relationships. Caco-2 cell experiments revealed highly cell-permeable compounds, and metabolic studies with **4** using rat liver microsomes showed sufficient stability.

Introduction

Aldosterone synthase (CYP11B2) is the key enzyme of mineralocorticoid biosynthesis. This cytochrome P450 enzyme catalyzes the conversion of its substrate, 11-deoxycorticosterone, to the mineralocorticoid aldosterone.[1] It is responsible for the regulation of the salt and water household and thus for the regulation of blood pressure. Besides the classical adrenal biosynthetic pathway, extra-adrenal sites of aldosterone production have been identified in brain, blood vessels, and heart.[2−4] Mineralocorticoid receptors have been detected in heart tissue, and it is known that aldosterone produced locally in the myocardium triggers myocardial fibrosis.[5,6] Thus, in addition to the indirect effects of aldosterone on the failing heart from sodium retention, hypervolemia, and hypertension, aldosterone exerts also direct effects on the heart. These findings show the importance of the blockade of aldosterone production as possible treatment for congestive heart failure and myocardial fibrosis. The mineralocorticoid receptor antagonists spironolactone and eplerenone (Rales and Ephesus study) were able to reduce mortality in heart failure patients and in patients after myocardial infarction.[7,8] The treatment with spironolactone, however, was accompanied by severe side effects because of its poor selectivity for the aldosterone receptor.[7,9] Additionally, a correlation between the use of spironolactone and hyperkalemia-associated mortality was observed.[10] Eplerenone turned out to be more selective, but the hyperkalemia problem can be expected to occur as well. In 1994, aldosterone synthase was already propagated as a novel pharmacological target by our group.[11] More recently, a new therapeutic option for the treatment of congestive heart failure and myocardial fibrosis was suggested by us: inhibition of aldosterone production using nonsteroidal, selective CYP11B2 inhibitors.[12,13] One of the main advantages of this approach is that nonsteroidal inhibitors are expected to have less side effects on the endocrine system than the steroidal antagonists. Furthermore, the inhibition of aldosterone formation should be more advantageous than interfering at the receptor level while leaving the elevated aldosterone levels unaffected. However, it is crucial that the inhibitors do not affect 11β-hydroxylase (CYP11B1), the key enzyme of the glucocorticoid biosynthesis, to avoid unwanted effects. It is quite a challenge to develop inhibitors with selectivity toward CYP11B2, since CYP11B1 and CYP11B2 have a sequence homology of more than 93%.[14]

Previously, we evaluated amidinohydrazones as potential CYP11B2 inhibitors using a CYP11B2-expressing yeast cell line and the adrenocortical tumor cell line NCI-H295R.[15] However, the compounds displayed almost no inhibitory activity toward CYP11B2. Recently, (imidazolyl- and pyridylmethylene)tetrahydronaphthalenes and -indanes **I** (Chart 1) were described as highly active and in some cases selective CYP11B2 inhibitors by our group.[16,17] By keeping the pharmacophore and rigidifying the molecules, a new class of 3-pyridine-substituted naphthalenes **II** was discovered, which turned out to be potent and selective inhibitors of CYP11B2.[18] The most interesting of these was the 6-methoxy-substituted naphthalene (IC_{50} CYP11B2 = 6 nM, IC_{50} CYP11B1 = 1577 nM, selectivity factor = 263).[18] Another way to make the pharmacophore rigid (compounds of type **III**) is examined in this paper. The synthesis of these compounds (Chart 2) and their biological activity toward the human CYP enzymes CYP11B2, CYP11B1, CYP17, and CYP19 are described. Molecular modeling and docking studies using our homology-modeled CYP11B2 structure[16−18] were performed to understand some interesting structure−activity relationships. Cell permeation properties of selected compounds using Caco-2 cells and metabolic stability of compound **4** using rat hepatic microsomes were also investigated.

* To whom correspondence should be addressed: phone + 49 681 302 3424; fax + 49 681 302 4386; e-mail rwh@mx.uni-saarland.de. Homepage: http://www.uni-saarland.de/fak8/hartmann/index.htm.
[†] Saarland University.
[‡] Max Planck Institute for Informatics.
[§] Pharmacelsus CRO.

10.1021/jm060055x CCC: $33.50
Published on Web 03/08/2006

Chart 1. Title Compounds **III** Derived from the Lead Compounds **I** and **II**

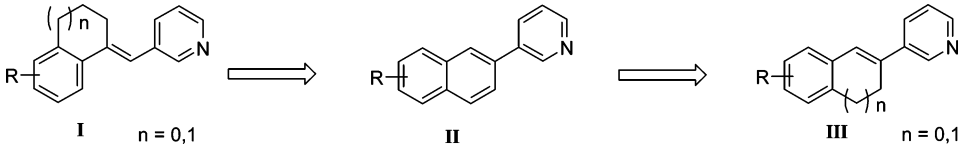

Chart 2. Title Compounds

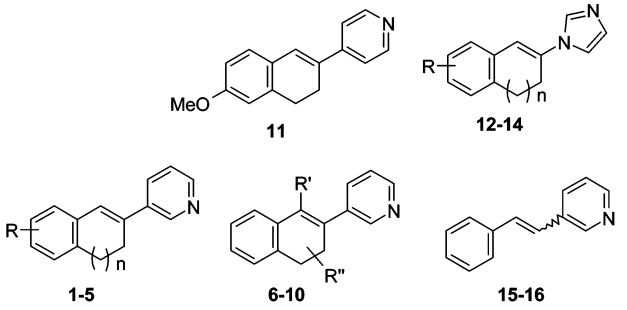

no	n	R	no	R'	R''	no	n	R
1	0	H	**6**	Me	H	**12**	0	H
2	1	H	**7**	Et	H	**13**	1	H
3	0	5-OMe	**8**	H	3-Me	**14**	1	6-OMe
4	1	6-OMe	**9**	H	4-Me	**15**	E-isomer	
5	1	7-OMe	**10**	H	4-Et	**16**	Z-isomer	

Scheme 1[a]

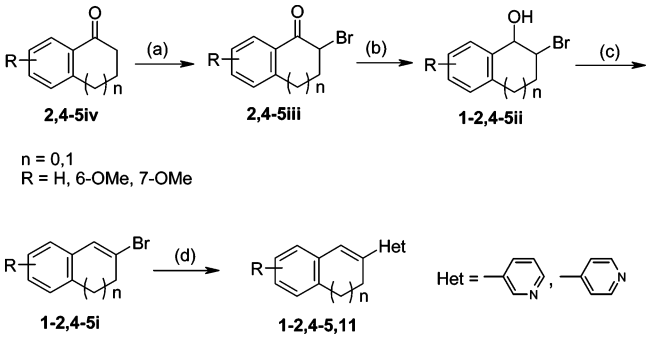

[a] Conditions: (a)TBA Br_3, CH_2Cl_2/MeOH, RT, 0.5−1 h; (b) $NaBH_4$, MeOH, 0 °C to RT, 1 h; (c) pTSA, toluene, reflux, 2 h; (d) 3- or 4-pyridylboronic acid, Na_2CO_3, $Pd(PPh_3)_4$, DME, 80 °C, 16 h.

Chemistry

The pyridine-substituted indenes and dihydronaphthalenes **1, 2**, **4, 5**, and **11** were synthesized by the route shown in Scheme 1. The α-bromoketones **2iii**, **4iii**, and **5iii**, synthesized by reacting the corresponding ketone **2iv**, **4iv**, or **5iv** with tetrabutylammonium tribromide at room temperature, were reduced with $NaBH_4$. The resulting alcohols **2ii**, **4ii**, and **5ii** and the commercially available 2-bromo-1-indanol **1ii** were refluxed in toluene with a catalytic amount of pTSA to yield the dehydrated compounds **1i**, **2i**, **4i**, and **5i**. The last step was the Suzuki cross-coupling with a 3- or 4-pyridylboronic acid in the presence of sodium carbonate and tetrakis(triphenylphosphine)palladium as a catalyst.[19] The intermediates **2iii**, **4iii**, and **5iii** and **1ii**, **2ii**, **4ii**, and **5ii** have one or two chiral centers. The resulting isomers were not separated and the racemic mixtures were used for the next reaction steps.

Scheme 2[a]

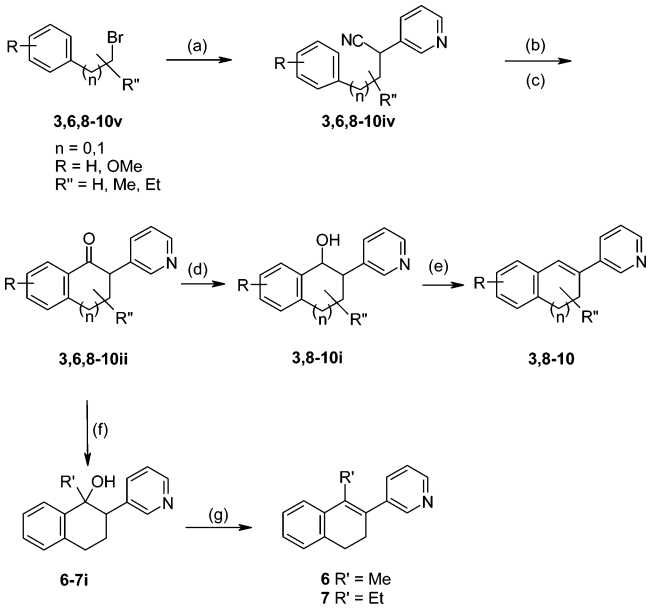

[a] Conditions: (a) 3-pyridylacetonitrile, $NaNH_2$, DMF, 0−80 °C, 6.5 h; (b) NaOH, EtOH, reflux, 24 h; (c) PPA, 110 °C, 20 min; (d) $NaBH_4$, MeOH, 0 °C to RT, 1 h; (e) CH_3COOH/H_2SO_4, 100 °C, 1 h; (f) R′MgX, toluene, reflux, 3 h; (g) HCl, 100 °C, 2 h.

An alternative synthetic route, based on the method by Bencze and Barsky,[20] was used for the synthesis of the 3-pyridine-substituted compounds **3** and **6**−**10** (Scheme 2). The alkylation of 3-pyridylacetonitrile with the brominated alkyl derivatives **3v**, **6v**, and **8v**−**10v** yielded the nitriles **3iv**, **6iv**, and **8iv**−**10iv**. Hydrolysis with NaOH resulted in the acids **3iii**, **6iii**, and **8iii**−**10iii**, which were cyclized to the corresponding indanones and tetralones **3ii**, **6ii**, and **8ii**−**10ii** by treatment with PPA. The reduction of the ketones **3ii** and **8ii**−**10ii** with $NaBH_4$ to the alcohols **3i** and **8i**−**10i** was followed by dehydration with sulfuric and acetic acids to give the desired indenes and dihydronaphthalenes **3** and **8**−**10**. The Grignard reaction of the tetralone **6ii** with an alkylmagnesium halogenide and subsequent dehydration of the resulting alcohols **6i** and **7i** with HCl yielded the 1-alkyl-substituted dihydronaphthalenes **6** and **7**. The isomers of the intermediates **3iv**, **6iv**, and **8iv**−**10iv** to **3i**, **6i**, and **8i**−**10i** were not separated but used as mixtures for the next reaction steps. The end products **8**−**10** were obtained as racemic mixtures.

The synthesis of the 1-imidazole-substituted indenes and dihydronaphthalenes **12**−**14** is shown in Scheme 3.[21] The α-bromoketones **2iii**, **4iii**, and **12iii** were stirred with imidazole for 24 h to give the imidazole-substituted ketones **12ii**−**14ii**. The reduction with $NaBH_4$ to the corresponding alcohols **12i**−**14i** and the subsequent acid-catalyzed dehydration yielded the 1-imidazolyl compounds **12**−**14**. The intermediates **12ii**−**14ii** and **12i**−**14i** were used as racemates or diastereomeric mictures, respectively. The (*E*)- and (*Z*)-3-styrylpyridines **15** and **16** were synthesized by a modified Wittig reaction (Scheme 4). The benzyl alcohol **15ii** was transformed into the phosphonium salt **15i**, which reacted with 3-pyridinecarbaldehyde in the presence of K_2CO_3 as a base and 18-crown-6 as phase-transfer catalyst.

Scheme 3[a]

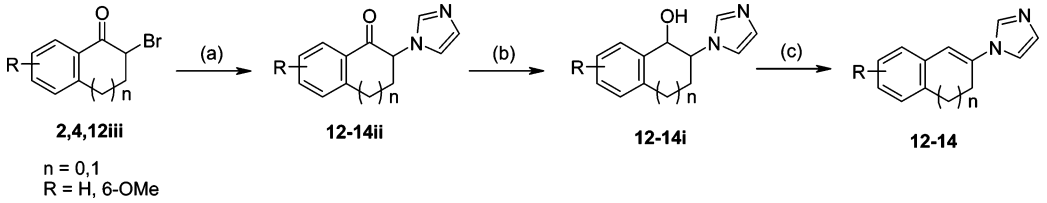

[a] Conditions: (a) imidazole, DMF, RT, 24 h; (b) $NaBH_4$, MeOH, 0 °C to RT, 1 h; (c) CH_3COOH, H_2SO_4, 100 °C, 1 h.

Scheme 4[a]

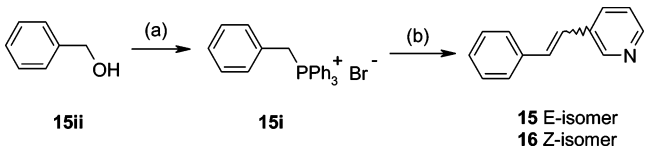

[a] Conditions: (a) PPh_3·HBr, benzene, reflux, 12 h; (b) 3-pyridinecarbaldehyde, K_2CO_3, 18-crown-6, CH_2Cl_2, reflux, 12 h.

The resulting *E*- and *Z*-isomers could be easily separated by column chromatography.

Biological Results

Inhibition of Human Adrenal Corticoids Producing CYP11B1 and CYP11B2 In Vitro (Table 1). For the determination of the inhibitory activity of our compounds toward human CYP11B2, our screening assay was used.[12] Human CYP11B2 expressing fission yeast was incubated with [^{14}C]deoxycorticosterone as substrate and the inhibitor at a concentration of 500 nM. The product formation was monitored by HPTLC using a phosphoimager.

Most of the 3-pyridine-substituted derivatives showed a higher inhibitory activity than the reference fadrozole (68%), an aromatase (CYP19) inhibitor that is in use for the treatment of breast cancer and is known to reduce aldosterone and cortisol levels in adrenal slices[22] and in vivo.[23] Only the 7-methoxy compound **5** exhibited a moderate activity (51%), and the racemic 4-ethyl-substituted 3,4-dihydronaphthalene **10** had little activity (20%). In general, the 3-pyridine-substituted indenes showed a slightly lower activity than the 3,4-dihydronaphthalenes. The shift of the methoxy substituent from 6- into 7-position of the 3,4-dihydronaphthalene core reduced activity, resulting in a moderate inhibitor **5**. Introduction of a methyl substituent in 1-, 3-, or 4-position of the 3,4-dihydronaphthalene moiety did not change potency (**6**, **8**, **9**), but a larger ethyl substituent in the 4-position resulted in a loss of activity (**10**). The 1-imidazolylnaphthalenes **12**−**14** and the ring open compounds **15** and **16** showed moderate activity (25−54%). The 4-pyridine-substituted dihydronaphthalene **11** had almost no activity (15%).

The most potent compounds, showing more than 60% inhibition in *Schizosaccharomyces pombe*, and a few less potent compounds were tested for activity and selectivity in V79 MZh cells expressing either CYP11B1 or CYP11B2.[12,24] [^{14}C]-Deoxycorticosterone was used as substrate, and the products were monitored as in the yeast assay. In Table 1 the IC_{50} values are presented. All the compounds with more than 60% inhibition in the yeast assay exhibited very high activity toward CYP11B2 with IC_{50} values in the range of 2−30 nM. They were also highly selective by showing only moderate inhibition of CYP11B1 (IC_{50} = 503−5684 nM). Compounds **1**, **2**, and **4** were over 180-fold more selective for CYP11B2 in contrast to the reference fadrozole, which displayed a selectivity factor of 10. The 5-methoxy-substituted indene **3** was the most selective compound with an exceptional selectivity factor of 1421.

Selected compounds with less than 60% inhibition in the yeast assay (**10**, **11**, **13**, **14**, and **16**) also showed only moderate or no activity at all in the CYP11B2 expressing V79 cells (IC_{50} values in the range between 176 and 2834 nM). An interesting finding is that the *Z*-isomer **16** exhibited some selectivity for CYP11B1 as compared to CYP11B2 with a 2.5-fold lower IC_{50} for the 11β-hydroxylase.

By use of V79 cells, selected compounds (**1**−**4**) were tested for their type of CYP11B2 inhibition. They turned out to be competitive inhibitors (in Figure 1, compound **3** is shown as an example) and revealed K_i values of 8.4, 4.6, 2.6, and 1.3 nM, respectively (K_M value of deoxycorticosterone = 185 nM).

Inhibition of Human CYP17, CYP19, and Hepatic CYPs in Vitro (Table 1). The selectivity of the compounds toward other steroidogenic CYP enzymes (CYP19, producing estrogens, and CYP17, forming androgens) was investigated. The IC_{50} values of the compounds for CYP19 were determined in vitro by use of human placental microsomes and [1-^{3}H]androstenedione as substrate as described by Thompson and Siiteri[25] with our modification.[26] All the compounds showed low or no inhibitory activity with IC_{50} values in the range between 814 and >36 000 nM, thus being much less active than the reference fadrozole (IC_{50} = 30 nM).

The percent inhibition values of the compounds toward CYP17 were determined in vitro with progesterone as substrate and the 50000*g* sediment of *Escherichia coli* recombinantly expressing human CYP17.[27,28] The indenes **1** and **3** and the 3- and 4-methyl-3,4-dihydronaphthalenes **8** and **9** displayed a weaker inhibition at a concentration of 2.5 μM than the reference ketoconazole (40%), which is an antimycotic and an unspecific inhibitor of several CYPs. The 3,4-dihydronaphthalenes **2**, **4**, and **7** showed similar or slightly higher inhibition (37−62%). The most potent CYP17 inhibitor was the 1-methyl-substituted compound **6**, exhibiting an IC_{50} value of 1085 nM. Thus, almost all of the tested compounds are very weak CYP17 inhibitors, having moderate to very low percent inhibition values that correspond to IC_{50} values of approximately 2500 nM or higher.

The most selective compound **3** with respect to CYP11B1 inhibition was further tested toward two crucial human hepatic CYP enzymes: CYP3A4, being responsible for 75% of the drug metabolism, and CYP2D6, for which a genetic polymorphism is described. Only marginal inhibitory effects could be observed (CYP3A4, ketoconazole IC_{50} = 50 nM, **3**, 7.0% ± 1.0% inhibition at 50 nM; CYP2D6, quinidine IC_{50} = 20 nM, **3**, 8.5% ± 2.2% inhibition at 20 nM)

Computational Results

Docking and protein modeling studies were performed to verify our homology-modeled CYP11B2 structure[16−18] and to explain interesting structure−activity relationships of two imidazolyl and one pyridyl compound (Table 2). Previously, compound **23** was found to be a highly active inhibitor of CYP11B2.[18] In this study, we observed that the corresponding dihydronaphthalene compound **13** shows a much lower activity.

Table 1. Inhibition of Human Adrenal CYP11B1 and CYP11B2, Human CYP17 and Human CYP19 In Vitro

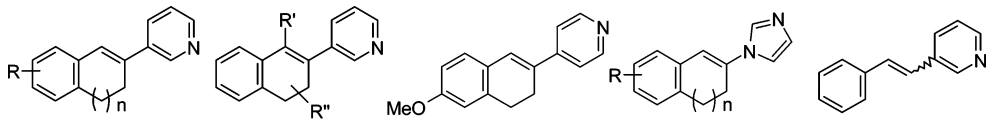

1-5 **6-10** **11** **12-14** **15-16**

					% inhibition[a]	IC_{50} value[b] (nM)		IC_{50} value[c] (nM)	% inhibition[d]	
compd	*n*	R	R′	R″	human[e] CYP11B2	V79 11B1[f] CYP11B1	V79 11B2[g] CYP11B2	human[h] CYP19	human[i] CYP17	selectivity[j] factor
1	0	H			90	2391	13	>36 000	2	184
2	1	H			95	1729	7	4073	37	247
3	0	5-OMe			66	5684	4	>36 000	7	1421
4	1	6-OMe			98	578	2	814	62	275
5	1	7-OMe			51	nd	45	nd	nd	
6			Me	H	94	1268	7	6045	69[k]	166
7			Et	H	81	2117	30	1507	57	71
8			H	3-Me	84	503	5	1787	27	97
9			H	4-Me	82	1291	13	3551	23	99
10			H	4-Et	20	1615	176	nd	nd	9
11					15	2529	2834	nd	nd	1
12	0	H			33	nd	448	nd	nd	
13	1	H			34	639	334	nd	nd	2
14	1	6-OMe			35	763	411	nd	nd	2
15		*E*-isomer			25	nd	nd	nd	nd	
16		*Z*-isomer			54	288	735	nd	nd	0.4
ketoconazole					36	224	81	40	nd	
fadrozole					68	10	1	30	5	10

[a] Mean value of four determinations, standard deviation less than 10%. [b] Mean value of four determinations, standard deviation less than 20%. nd = not determined. [c] Mean value of four determinations, standard deviation less than 5%. [d] Mean value of four determinations, standard deviation less than 10%. nd = not determined. [e] *S. pombe* expressing human CYP11B2; substrate deoxycorticosterone, 100 nM; inhibitor, 500 nM. [f] Hamster fibroblasts expressing human CYP11B1; substrate deoxycorticosterone, 100 nM. [g] Hamster fibroblasts expressing human CYP11B2; substrate deoxycorticosterone, 100 nM. [h] Human placental CYP19; 1 mg/mL protein; substrate androstenedione, 500 nM. [i] *E.coli* expressing human CYP17; 5 mg/mL protein; substrate progesterone, 2.5 μM; inhibitor, 2.5 μM. [j] IC_{50} CYP11B1/IC_{50} CYP11B2. [k] IC_{50} CYP17 = 1085 nM.

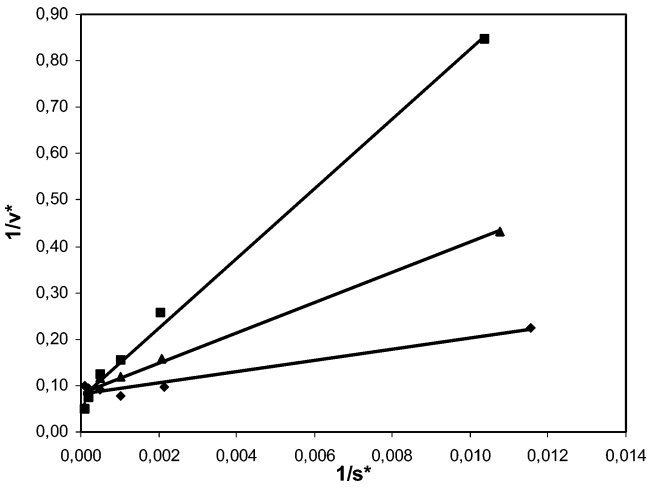

Figure 1. Lineweaver−Burk plot of **3** indicating competitive type of inhibition: (◆) no inhibitor; (▲) **3**, 3 nM; (■) **3**, 15 nM.

However, its corresponding pyridyl compound **2** is again highly active. To explain this interesting phenomenon, compounds **2**, **13**, and **23** were docked into the CYP11B2 model and the structural and energetic aspects of the protein−inhibitor interactions of the energetically most favorable docked complexes were analyzed. Subsequently the dynamics of the complexes were studied through molecular dynamics simulations of the docked complexes. In Figure 2, the best scoring docking poses for the three compounds are shown. The ligand−protein interactions are indicated by green lines. Figure 2b shows the least active compound **13**. In addition to the Fe−N interaction with the heme group, it forms aromatic−hydrophobic interactions between its phenyl and imidazolyl ring and the binding pocket amino acids Leu227/Phe231 and Leu382/Thr318. Due to the imidazolyl/

Table 2. IC_{50} Values for CYP11B2 Inhibition of Selected Compounds

Compd	Structure	IC_{50}-value (nM) V79 11B2 CYP11B2
2	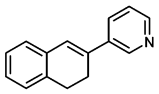	7
13	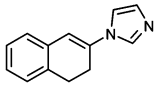	334
23	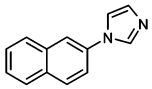	39

amino acid side-chain interactions, a distortion of the Fe−N binding geometry can be observed. The corresponding highly active naphthalene compound **23**, shown in Figure 2c, obviously forms phenyl−CH_3 interactions with both aromatic rings of the naphthalene and Leu382, Thr318, Leu227, and Phe231. However, the imidazole moiety is forming only the Fe−N interaction, and no distortion of the Fe−N binding geometry by interactions with binding pocket residues was found. In Figure 2a, the docked complex of compound **2** is presented. Its binding pattern is the same as for compound **13**. However, due to the larger size of the pyridine ring and the different geometry, the dihydronaphthalene moiety of the inhibitor is placed differently in the pocket, leading to interactions with other amino acids (Val129 and Ala313 instead of Leu227, Phe231, and Leu382). Its Fe−N interaction is not distorted as it is with compound **13**. The main difference between the binding patterns of compounds **2**/**23** and compound **13** is the distortion of the Fe−N

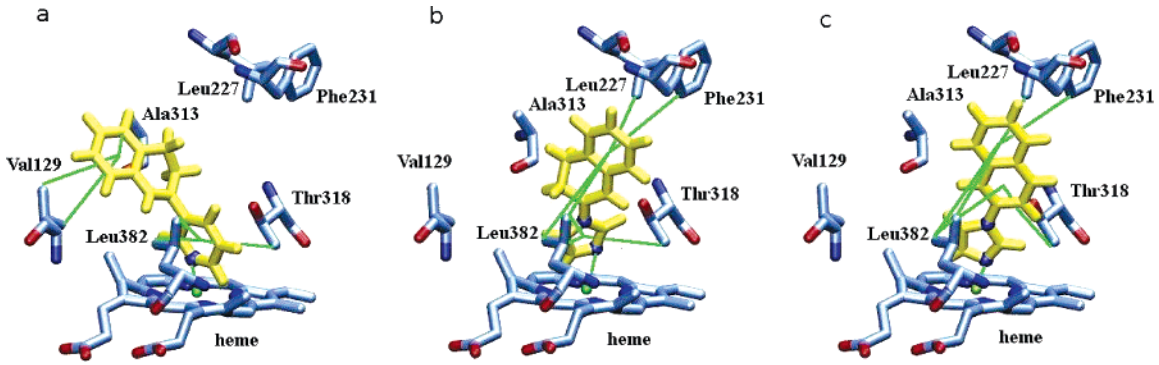

Figure 2. Structure of the CYP11B2 binding pocket with the docked inhibitors **2** (a), **13** (b), and **23** (c). The structures shown correspond to the docking poses with the lowest energy score, and all amino acids of the binding pocket that interact with the inhibitors are given. The inhibitors are presented in yellow, nitrogen atoms are colored blue, and oxygen atoms are in red. The green lines correspond to the protein−inhibitor interactions found by FlexX.

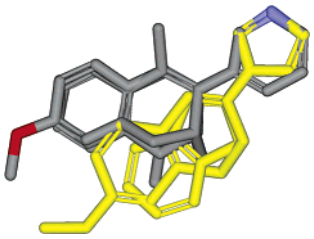

Figure 3. Superimposition of the pyridine-substituted compounds **2**, **4**, **6**, **8**, and **9** (gray) and the imidazole-substituted compounds **12**−**14** (yellow).

interaction in the latter case, which indicates that this might be the main reason for the lower activity of compound **13**.

The same tendency as observed for the IC_{50} values (Table 2) can be seen for the energy scores of the docking poses shown in Figure 2, which are −50.137 for compound **2**, −42.739 for compound **13**, and −48.116 for compound **23**. However, these energies cannot solely explain the large difference in the IC_{50} values of compounds **2**/**23** and compound **13**. Obviously, not static interactions alone but also the dynamics of the system must be considered. Consequently, molecular dynamics simulations were performed for the docked complexes of compounds **2** and **13**. Identical simulations had been carried out for compound **23** in a previous study,[18] and a correlation between the stability of the docked poses during molecular dynamics simulations and the IC_{50} values of **23** and other inhibitors was observed. These results were confirmed in the present work: During the 1 ns simulations, compound **13** moved away (∼4 Å) from the heme cofactor, whereas compound **2** stayed close to its docked position, as did compound **23** in the previous work.[18] This separates the three complexes in two classes: compound **2** and **23** form a strong and dynamically stable Fe−inhibitor interaction, whereas compound **13** does not. To further explain the differences in the orientation of the pyridyl and imidazolyl compounds in the binding pocket, superimposition of these two classes of compounds was performed. From Figure 3 it is clear that when the lone pairs of the heterocyclic nitrogens are pointing in the same direction, the corresponding dihydronaphthalene cores are located with a different angle toward the plane of the heme.

Caco-2 Cell Permeability Screening and Metabolic Stability. Selected compounds (**1**−**4** and **6**−**9**) that showed high CYP11B2 inhibitory activity and selectivity toward other CYP enzymes were further screened for cell permeability properties on Caco-2 monolayers. The Caco-2 cells are a human epithelial colon carcinoma cell line and a suitable in vitro model for the evaluation of intestinal absorption of drugs.[29] To increase the throughput of the Caco-2 assay, a multiple dosing approach was used for the test compounds. Compound mixtures are administered, and by use of reference compounds,[29−32] the inhibitors can be classified as having low, medium, or high cell-permeability. All the tested compounds had medium to high cell permeability with P_{app} values in the range between 3.4 and 15.1 × 10^{-6} cm/s (Table 3).

Table 3. Caco-2 Cell Permeation of Highly Active and Selective CYP11B2 Inhibitors by a Multiple Dosing Approach

compd	P_{app} (×10^{-6} cm/s)[a,b] multiple dosing ± SD
1	6.6 ± 0.5
2	14.6 ± 0.6
3	12.5 ± 0.2
4	13.5 ± 0.6
6	3.4 ± 0.1
7	21.6 ± 1.6
8	14.7 ± 0.6
9	16.3 ± 3.0
atenolol	0.1 ± 0.03
ketoprofene	25.7 ± 0.5
testosterone	9.4 ± 0.2
erythromycin	<LOD

[a] Permeability of research compounds was classified according to described reference compounds: testosterone[29] (high), atenolol[30] (low), ketoprofene[31] (high), and erythromycin[32] (not detectable). [b] Mean value of three determinations.

The 6-methoxydihydronaphthalene **4**, a highly active and selective CYP11B2 inhibitor with favorable cell permeability properties, was selected to be further tested for its metabolic stability in rat liver microsomes. Samples were taken at various time points to determine the remaining parent compound. The assay showed that compound **4** has a half-life of 67 min, which is an indication that the compound shows reasonable stability.

By use of the supernatant of the incubation, the major metabolites of compound **4** were isolated and characterized by liquid chromatography−tandem mass spectrometry (LC-MS/MS). The fragmentation of the metabolite with $[M + H]^+$ at *m*/*z* 224 suggests that **4** has undergone O-demethylation, resulting in the formation of the corresponding naphthol. Two other major metabolites with $[M + H]^+$ at *m*/*z* 254 bear an additional oxygen atom in their dihydronaphthalene structure.

Discussion and Conclusion

Recently, we had reported that 3-pyridyl-substituted naphthalenes (**II**, Chart 1) are potent and selective CYP11B2 inhibitors.[18] In this study, it is demonstrated that, in the class of pyridyl- and 1-imidazolyldihydronaphthalenes and −indenes, even more potent and selective compounds could be discovered.

The dihydronaphthalene compounds exhibited in general a slightly higher activity than the corresponding indenes. The 3-pyridyl compounds exceeded the imidazolyl compounds and especially the 4-pyridyl derivative. The most active inhibitor, compound **4**, exhibited a very low IC_{50} value of 2 nM. It is the most potent compound described so far. The methoxy-substituted indene **3** was very potent (IC_{50} value of 4 nM) and the most selective compound toward CYP11B1. It showed an extraordinary selectivity factor of 1421, which is very remarkable since the amino acid homology between CYP11B2 and B1 is more than 93%.[14] Compound **3** affects the hepatic CYP enzymes CYP3A and CYP2D6 only marginally and, just like the other compounds of this paper, shows inhibition of the other steroidogenic CYP enzymes, CYP17 and CYP19, only at very high concentrations. Interestingly, compound **16** turned out to be a slightly selective CYP11B1 inhibitor, being 2.5 times more active toward CYP11B1 than CYP11B2. CYP11B1 inhibitors could be used for the treatment of Cushing's syndrome and metabolic syndrome.

Docking studies with compounds **2**, **13**, and **23** using our CYP11B2 protein model led to interesting observations. The imidazolyl-substituted dihydronaphthalene compound **13**, which is a less active inhibitor, shows a different binding behavior than the corresponding naphthalene compound **23**. The dihydronaphthalene moiety forms less interactions with the protein than the naphthalene ring. On the other hand, additional aromatic−hydrophobic interactions are observed for the imidazole ring of compound **13**. To form these interactions, the heterocycle is shifted with respect to the heme plane, weakening the Fe−N interaction. For strong inhibitor binding, the directionality of the Fe−N interaction must be almost perpendicular with respect to the plane of the heme. As a result of the distortion of this interaction, **13** cannot bind as strongly as the others and is less active. Due to the different geometry of the pyridyl compounds, the dihydronaphthalene compound **2** is docked differently, leading to a much smaller distortion of the Fe−N interaction than is observed for **13**. These findings are confirmed by the energy scores of the docked poses.

Looking at the ligand−protein interactions in our homology model, it is obvious that there exists a specific "network" of hydrophobic groups in the binding pocket, which are important for interaction and which have to be complemented by the inhibitor in a way that the geometry of the Fe−N interaction is retained. Strong binding is possible only in this case. This is very interesting, because such specific interactions normally consist of hydrogen bonds and the hydrophobic interactions are supposed to play only a minor role for the exact positioning of the ligand. In addition, our dynamics studies indicate that small differences in this interaction network can lead to large differences in the dynamics of the system. Thus, studying the dynamics of the docked complexes, we could clearly distinguish between strong (compounds **2** and **23**) and weak (compound **13**) inhibitors.

Cell permeation screening using Caco-2 cells showed that the 3-pyridine-substituted dihydronaphthalenes and indenes are highly cell-permeable. This is an indication that these compounds might be perorally available. A metabolic stability test using rat hepatic microsomes revealed that the highly active compound **4** shows a reasonable metabolic stability with a half-life time of 67 min. Presently this compound is being further investigated for its in vivo activity.

We expect a reduction of the plasma aldosterone level by these compounds since FAD286—one enantiomer of the racemic fadrozole—was recently shown to reduce circulating and cardiac aldosterone levels in transgenic rats overexpressing human renin and angiotensinogen genes.[33]

Experimental Section

Chemical Methods. Melting points were measured on a Mettler FP1 melting point apparatus and are uncorrected. IR spectra were measured neat on a Bruker Vector 33FT-infrared spectrometer. ^{1}H NMR spectra were recorded on a Bruker DRX-500 (500 MHz) instrument. Chemical shifts are given in parts per million (ppm), and tetramethylsilane (TMS) was used as internal standard for spectra obtained in $CDCl_3$. All coupling constants (J) are given in hertz. Mass spectra (electrospray ionization (ESI)) were measured on a TSQ quantum (Thermo Electron Corporation) instrument. Elemental analyses were performed at the Department of Instrumental Analysis and Bioanalysis, Saarland University. Reagents and solvents were used as obtained from commercial suppliers without further purification. Column chromatography (CC) was performed on silica gel (70−200 μm), and the reaction progress was determined by thin-layer chromatography (TLC) analyses on Alugram SIL G/UV_{254} (Macherey-Nagel).

The following compounds were prepared according to previously described procedures: 2-bromo-1*H*-indene (**1i**),[34] [1-(bromomethyl)-propyl]benzene (**10v**),[35] 3-pyridylboronic acid,[36] and 4-pyridylboronic acid.[36]

General Procedure for Synthesis of Compounds 2iii, 4iii, 5iii, and 12iii. To a solution of ketone (11.75 mmol) in dichloromethane/methanol (140 mL/56 mL) was added $TBABr_3$ (12.92 mmol) at room temperature. The mixture was stirred until decoloration of the orange solution took place. The solvent was removed in vacuo and the obtained solid was extracted with diethyl ether. The ether layer was dried ($MgSO_4$), filtered, and evaporated in vacuo.

2-Bromo-3,4-dihydro-2*H*-naphthalen-1-one (2iii). Purification by CC (CH_2Cl_2); yield 50%. ^{1}H NMR ($CDCl_3$) δ 2.45−2−57 (m, 2H, H-4), 2.92 (dt, 1H, ^2J = 17.0 Hz, ^3J = 4.4 Hz, H-3), 3.29−3.36 (m, 1H, H-3′), 4.73 (t, 1H, ^3J = 4.4 Hz, H-2), 7.28 (d, 1H, ^3J = 7.6 Hz, Ar H), 7.36 (t, 1H, ^3J = 7.6 Hz, Ar H), 7.52 (td, 1H, ^3J = 7.6 Hz, ^4J = 1.3 Hz, Ar H), 8.10 (dd, 1H, ^3J = 7.9 Hz, ^4J = 1.3 Hz, Ar H). IR (cm^{-1}): ν_{max} 3069, 2933, 1665, 1595.

2-Bromo-6-methoxy-3,4-dihydro-2*H*-naphthalen-1-one (4iii). No purification; yield 95%.

2-Bromo-7-methoxy-3,4-dihydro-2*H*-naphthalen-1-one (5iii). Purification by CC (CH_2Cl_2); yield 60%.

2-Bromoindan-1-one (12iii). Purification by CC (CH_2Cl_2); yield 78%.

General Procedure for Synthesis of Compounds 2ii, 4ii, and 5ii. A solution of the α-bromoketone (1.77 mmol) in anhydrous methanol/tetrahydrofuran (1/1.6 mL) was stirred under nitrogen atmosphere in an ice bath. $NaBH_4$ (1.24 mmol) was added portionwise. After being stirred for 15 min at 0 °C and 0.5 h at room temperature, the mixture was poured into water and extracted with diethyl ether. The organic layer was dried ($MgSO_4$), filtered, and evaporated in vacuo. This compound was used for further reaction without purification.

2-Bromo-1, 2, 3, 4-tetrahydronaphthalen-1-ol (2ii). Yield 88%. ^{1}H NMR ($CDCl_3$) δ 2.28−2.34 (m, 1H, H-3), 2.50−2.57 (m, 1H, H-3′), 2.86−2.92 (m, 1H, H-4), 3.01−3.15 (m, 1H, H-4′), 4.71−4.74 (m, 1H, H-2), 4.81 (d, 1H, ^3J = 3.5 Hz, H-1), 7.12−7.14 (m, 1H, Ar H), 7.25−7.28 (m, 2H, Ar H), 7.49−7.50 (m, 1H, Ar H). IR (cm^{-1}): ν_{max} 3413, 3022, 2955, 2923, 2849, 1603, 1490, 1455, 1225.

2-Bromo-6-methoxy-1,2,3,4-tetrahydro-naphthalen-1-ol (4ii). Yield 86%.

2-Bromo-7-methoxy-1,2,3,4-tetrahydro-naphthalen-1-ol (5ii). Yield 84%.

General Procedure for Synthesis of Compounds 1i, 2i, 4i, and 5i. A mixture of the alcohol (2.44 mmol) and *p*-toluenesulfonic acid (0.24 mmol) in 10 mL of toluene was heated at reflux (with Dean-Starktrap) for 2 h to remove any water. The mixture was washed with saturated sodium bicarbonate and water. The organic layer was dried ($MgSO_4$), filtered, and evaporated in vacuo.

2-Bromo-1*H*-indene (1i). Purification by CC (hexane); yield 47%. ^{1}H NMR ($CDCl_3$) δ 3.61 (s, 2H, H-3), 6.94 (t, 1H, ^4J = 1.9 Hz, H-1), 7,17 (td, 1H, ^3J = 7.6 Hz, ^4J = 1.3 Hz, Ar H), 7.24 (t, 1H, ^3J = 7.6 Hz, ArH), 7.31 (d, 1H, ^3J = 7.6 Hz, Ar H), 7.38 (d, 1H, ^3J = 7.6 Hz, Ar H). IR (cm^{-1}): ν_{max} 3072, 2897, 1556.

3-Bromo-1,2-dihydronaphthalene (2i). Purification by CC (hexane); yield 81%.

3-Bromo-7-methoxy-1,2-dihydronaphthalene (4i). Purification by CC (hexane/EtOAc, 80:20); yield 60%.

3-Bromo-6-methoxy-1,2-dihydronaphthalene (5i). Purification by CC (hexane/EtOAc, 80:20); yield 58%.

General Procedure for Synthesis of Compounds 1, 2, 4, 5, and 11. A mixture of the bromo compound (2.02 mmol), 3- or 4-pyridylboronic acid (2.63 mmol), sodium carbonate (4.24 mmol), and tetrakis(triphenylphosphine)palladium (0.04 mmol) in 15 mL of ethylene glycol dimethyl ether was heated at 80 °C overnight under a nitrogen atmosphere. The mixture was cooled to room temperature and water was added. The mixture was extracted with dichloromethane and the organic layer was dried ($MgSO_4$), filtered, and evaporated in vacuo.

3-(1*H*-Inden-2-yl)pyridine (1). Purification by CC (CH_2Cl_2/MeOH, 99:1); yield 51%, mp 102 °C. ^{1}H NMR ($CDCl_3$): δ = 3.81 (s, 2H, H-3), 7.23 (td, 1H, ^3J = 7.2 Hz, ^4J = 0.9 Hz, Ar H), 7.29−7.32 (m, 3H, H-1, Ar H, pyr H-5), 7.44 (d, 1H, ^3J = 7.2 Hz, Ar H), 7.50 (d, 1H, ^3J = 7.2 Hz, Ar H), 7.89 (dt, 1H, ^3J = 8.1 Hz, ^4J = 1.9 Hz, pyr H-4), 8.50 (s, 1H, pyr H-6), 8.90 (s, 1H, pyr H-2). IR (cm^{-1}): ν_{max} 3054, 2916, 1533. MS *m/z* 194 (MH^+). Anal. ($C_{14}H_{11}N$) C, H, N.

3-(3,4-Dihydronaphthalen-2-yl)pyridine (2). Purification by CC (CH_2Cl_2/MeOH, 97:3); yield 62%.

3-(6-Methoxy-3,4-dihydronaphthalen-2-yl)pyridine (4). Purification by CC (CH_2Cl_2/MeOH, 99:1); yield 89%.

3-(7-Methoxy-3,4-dihydronaphthalen-2-yl)pyridine (5). The reaction was stirred for 2 h. Purification by CC (CH_2Cl_2/MeOH, 99:1); yield 79%.

4-(6-Methoxy-3,4-dihydronaphthalen-2-yl)pyridine (11). The reaction was stirred for 2 h. Purification by CC (CH_2Cl_2/MeOH, 97:3); yield 51%.

General Procedure for Synthesis of Compounds 3iv, 6iv, and 8iv−10iv. To a suspension of $NaNH_2$ (9.40 mmol) in 20 mL of anhydrous dimethylformamide (three-neck flask, reflux cooler, gas inlet and dropping funnel with septum) under nitrogen was added dropwise 3-pyridylacetonitrile (8.46 mmol) while the reaction mixture was stirred and cooled with an ice bath. After being stirred for 1 h at room temperature and 1 h at 80 °C, the mixture was cooled with an ice bath and the corresponding brominated alkyl derivative **3v**, **6v**, or **8v−10v** (7.99 mmol) was added dropwise. The reaction was stirred for 3 h at room temperature and then 1 h at 80 °C. After cooling, an excess of water was added and the mixture was extracted with diethyl ether. The organic layer was washed with water, dried ($MgSO_4$), filtered, and evaporated in vacuo. The product was purified by column chromatography and eluted with CH_2Cl_2/MeOH (99:1).

3-(3-Methoxyphenyl)-2-pyridin-3-ylpropionitrile (3iv). Yield 26%. ^{1}H NMR ($CDCl_3$) δ 3.13−3.25 (m, 2H, H-3), 3.76 (s, 3H, OCH_3), 4.20 (t, 1H, ^3J = 7.2 Hz, H-2), 6.65 (t, 1H, ^4J = 2.2 Hz, Ar H), 6.67 (d, 1H, ^3J = 7.6 Hz, Ar H), 6.82 (dd, 1H, ^3J = 8.2 Hz, ^4J = 2.2 Hz, Ar H), 7.21 (t, 1H, ^3J = 8.2 Hz, Ar H), 7.43−7.46 (m, 1H, pyr H-5), 7,74 (dt, 1H, ^3J = 8.2 Hz, ^4J = 1.9 Hz, pyr H-4), 8.61 (d, 1H, ^4J = 2.5 Hz, pyr H-2), 8.62 (dd, 1H, ^3J = 5.0 Hz, ^4J = 1.6 Hz, pyr H-6). IR (cm^{-1}): ν_{max} 3030, 2938, 2837, 2244, 1602, 1491, 1264.

4-Phenyl-2-pyridin-3-ylbutyronitrile (6iv). Yield 47% (mixture of stereoisomers).

3-Methyl-4-phenyl-2-pyridin-3-ylbutyronitrile (8iv). Yield 29% (mixture of stereoisomers).

4-Phenyl-2-pyridin-3-ylpentanenitrile (9iv). Yield 25% (mixture of stereoisomers).

4-Phenyl-2-pyridin-3-ylhexanenitrile (10iv). Purification by CC (CH_2Cl_2/MeOH, 98:2); yield 59%.

General Procedure for Synthesis of Compounds 3iii, 6iii, and 8iii−10iii. To a solution of the nitrile compound (2.04 mmol) in 3 mL of ethanol was added sodium hydroxide (22.46 mmol) in 1 mL of water. After reflux for 24 h, some water was added and the pH was adjusted to 5 with 2 N HCl solution and aqueous acetic acid. The mixture was extracted with ethyl acetate and, after drying ($MgSO_4$) and filtration, evaporated in vacuo. This compound was used for further reaction without purification.

3-(3-Methoxyphenyl)-2-pyridin-3-ylpropionic acid (3iii). Yield 99%. IR (cm^{-1}): ν_{max} 2939, 2836, 2526, 1721, 1585, 1491.

4-Phenyl-2-pyridin-3-ylbutyric acid (6iii). Yield 74%.

3-Methyl-4-phenyl-2-pyridin-3-ylbutyric acid (8iii). Yield 99%.

4-Phenyl-2-pyridin-3-ylpentanoic acid (9iii). Yield 68%.

4-Phenyl-2-pyridin-3-ylhexanoic acid (10iii). Yield 99%.

General Procedure for Synthesis of Compounds 3ii, 6ii, and 8ii−10ii. A mixture of polyphosphoric acid (2.2 g) and the acid (0.53 g, 2.05 mmol) was stirred at 110 °C for 20 min. The reaction was poured into ice water and neutralized with 6% NaOH solution. The pH was adjusted to 8 with sodium bicarbonate, and the solution was extracted with diethyl ether. The organic layer was dried ($MgSO_4$), filtered, and evaporated in vacuo.

5-Methoxy-2-pyridin-3-ylindan-1-one (3ii). Purification by CC (CH_2Cl_2/MeOH, 97:3); yield 48%. ^{1}H NMR ($CDCl_3$) δ 3.20 (dd, 1H, ^2J = 17.3 Hz, ^3J = 4.1 Hz, H-3), 3.67 (dd, 1H, ^2J = 17.3 Hz, ^3J = 8.5 Hz, H-3′), 3.90−3.92 (m, 4H, OCH_3, H-2), 6.96−6.98 (m, 2H, Ar H), 7.28−7.31 (m, 1H, pyr H-5), 7,57 (dt, 1H, ^3J = 8.2 Hz, ^4J = 1.9 Hz, pyr H-4), 7.74 (d, 1H, ^3J = 8.2 Hz, Ar H), 8.50−8.51 (m, 2H, pyr H-6, pyr H-2). IR (cm^{-1}): ν_{max} 2945, 2841, 1702, 1599, 1261.

2-Pyridin-3-yl-3,4-dihydro-*2H*-naphthalen-1-one (6ii). Purification by CC (CH_2Cl_2/MeOH, 98:2); yield 90%.

3-Methyl-2-pyridin-3-yl-3,4-dihydro-*2H*-naphthalen-1-one (8ii). Purification by CC (CH_2Cl_2/MeOH, 96:4); yield 38% (mixture of stereoisomers).

4-Methyl-2-pyridin-3-yl-3,4-dihydro-*2H*-naphthalen-1-one (9ii). Purification by CC (CH_2Cl_2/MeOH, 99:1); yield 98% (mixture of stereoisomers).

4-Ethyl-2-pyridin-3-yl-3,4-dihydronaphthalen-1(2*H*)-one (10ii). Purification by CC (CH_2Cl_2/MeOH, 97:3); yield 63% (mixture of stereoisomers).

General Procedure for Synthesis of Compounds 3i and 8i−10i. A solution of the ketone (1.77 mmol) in 5 mL of anhydrous methanol was stirred under nitrogen in an ice bath. $NaBH_4$ (3.54 mmol) was added portionwise. After being stirred for 1 h at room temperature, the mixture was poured into water and extracted with dichloromethane. The organic layer was dried ($MgSO_4$), filtered, and evaporated in vacuo. The resulting alcohol was used for further reaction without purification.

5-Methoxy-2-pyridin-3-ylindan-1-ol (3i). Yield 53%.

3-Methyl-2-pyridin-3-yl-1,2,3,4-tetrahydronaphthalen-1-ol (8i). Yield 72%.

4-Methyl-2-pyridin-3-yl-1,2,3,4-tetrahydronaphthalen-1-ol (9i). Yield 45%.

4-Ethyl-2-pyridin-3-yl-1,2,3,4-tetrahydronaphthalen-1-ol (10i). Yield 98%.

General Procedure for Synthesis of Compounds 3 and 8−10. A mixture of 1 mL of acetic acid, 0.14 mL of sulfuric acid, and the alcohol (0.30 mmol) was stirred at 100 °C for 1 h. The reaction was poured into ice water and basified with a 6% sodium hydroxide solution. After extractions with dichloromethane, the organic layer was dried ($MgSO_4$), filtered, and evaporated *in* vacuo. The product was purified by column chromatography, eluting with CH_2Cl_2/MeOH (98:2).

3-(6-Methoxy-1*H*-inden-2-yl)pyridine (3). Yield 45%, mp 82 °C. ^{1}H NMR ($CDCl_3$) δ 3.77 (s, 2H, H-3), 3 85 (s, 3H, OCH_3), 6.86 (dd, 1H, ^3J = 8.2 Hz, ^4J = 2.2 Hz, Ar H), 7.09 (d, 1H,^4J = 1.5 Hz, Ar H), 7.30 (s, 1H, H-1), 7.34 (d, 1H, ^3J = 8.2 Hz, Ar H), 7.36−7.39 (m, 1H, pyr H-5), 7.94 (dt, 1H, ^3J = 7.9 Hz, ^4J = 1.5 Hz, pyr H-4), 8.46 (dd, 1H, ^3J = 4.9 Hz, ^4J = 1.5 Hz, pyr H-6), 8.85 (d, 1H, ^4J = 1.8 Hz, pyr H-2). IR (cm^{-1}): ν_{max} 3059, 2905,

2836, 1685, 1607, 1493, 1259. MS *m*/*z* 224 (MH^+). Anal. ($C_{15}H_{13}NO \cdot 0.09H_2O$) C, H, N.

3-(3-Methyl-3,4-dihydronaphthalen-2-yl)pyridine (8). Yield 63%, mp 169 °C (HCl salt).

3-(4-Methyl-3,4-dihydronaphthalen-2-yl)pyridine (9). Yield 51%, mp 189 °C (HCl salt).

3-(4-Ethyl-3,4-dihydronaphthalen-2-yl)pyridine (10). Yield 55%, mp 174 °C (HCl salt).

General Procedure for Synthesis of Compounds 6i and 7i. To a solution of 2-pyridin-3-yl-3,4-dihydronaphthalen-1-one **6ii** (0.15 g, 0.65 mmol) in 15 mL of dry toluene was added alkylmagnesium chloride (3 M) in THF (0.44 mL, 1.31 mmol) dropwise under nitrogen atmosphere. After the mixture was stirred at reflux for 3 h and at room temperature overnight, an ammonium chloride solution was added. The mixture was extracted with ethyl acetate, dried ($MgSO_4$), filtered, and evaporated in vacuo.

1-Methyl-2-pyridin-3-yl-1,2,3,4-tetrahydronaphthalen-1-ol (6i). Purification by CC (CH_2Cl_2/MeOH, 98:2); yield 41%. ^{1}H NMR ($CDCl_3$) δ 1.07 (s, 3H, CH_3), 2.04−2.08 (m, 1H, H-3), 2.25−2.31 (m, 1H, H-3′), 2.96−2.30 (m, 2H, H-4), 3.28−3.31 (m, 2H, H-2, OH), 7.03 (d, 1H, ^3J = 7.9 Hz, Ar H), 7.12 (t, 1H, ^3J = 7.9 Hz, Ar H), 7.17 (t, 1H, ^3J = 7.9 Hz, Ar H), 7.56 (d, 1H, ^3J = 7.9 Hz, Ar H), 7.69−7.71 (m, 1H, pyr H-5), 8.14 (d, 1H, ^3J = 7.9 Hz, pyr H-4), 8.54 (d, 1H, ^3J = 5.4 Hz, pyr H-6), 8.65 (s, 1H, pyr H-2). IR (cm^{-1}): ν_{max} 3316, 3065, 2934, 1687, 1603, 1428.

1-Ethyl-2-pyridin-3-yl-1,2,3,4-tetrahydronaphthalen-1-ol (7i). Purification by CC (CH_2Cl_2/MeOH, 99:1); yield 20%.

General Procedure for Synthesis of Compounds 6 and 7. A mixture of 1 mL of HCl and the alcohol (0.30 mmol) was stirred at 100 °C for 2 h. The reaction was poured into ice water and basified with a 6% sodium hydroxide solution. After extractions with dichloromethane, the organic layer was dried ($MgSO_4$), filtered, and evaporated in vacuo.

3-(1-Methyl-3,4-dihydronaphthalen-2-yl)-pyridine (6). Purification by CC (CH_2Cl_2/MeOH, 97:3); yield 63%, mp 174 °C (HCl salt). ^{1}H NMR ($CDCl_3$) δ 2.05 (s, 3H, CH_3), 2.57 (td, 2H, ^3J = 8.2 Hz, ^4J = 1.6 Hz, H-3), 2.92 (t, 2H, ^3J = 8.2 Hz, H-4), 7.19−7.23 (m, 2H, Ar H), 7.27 (t, 1H, ^3J = 7.6 Hz, Ar H), 7.38 (d, 1H, ^3J = 7.6 Hz, Ar H), 7.41−7.45 (m, 1H, pyr H-5), 7.72 (td, 1H, ^3J = 7.92 Hz, ^4J = 1.6 Hz, pyr H-4), 8.54 (dd, 1H, ^3J = 5.0 Hz, ^4J = 1.6 Hz, pyr H-6), 8.57 (s, 1H, pyr H-2). IR (cm^{-1}): ν_{max} 3024, 2937, 2831, 1602, 1487, 1408, 1250. MS *m*/*z* 222 (MH^+). Anal. ($C_{16}H_{15}N \cdot HCl \cdot 0.19H_2O$) C, H, N.

3-(1-Ethyl-3,4-dihydronaphthalen-2-yl)-pyridine (7). Purification by CC (CH_2Cl_2/MeOH, 99:1); yield 60%, mp 141 °C (HCl salt).

General Procedure for Synthesis of Compounds 12ii−14ii. A solution of α-bromoketone (4.79 mmol) and imidazole (23.94 mmol) in 20 mL of DMF was stirred overnight at room temperature. The mixture was poured into ice water and extracted with dichloromethane. After exhaustive washing with water, the organic layer was dried ($MgSO_4$), filtered, and evaporated in vacuo. The product was purified by column chromatography and eluted with CH_2Cl_2/MeOH (98:2).

2-(1*H*-Imidazol-1-yl)indan-1-one (12ii). Yield 39%, mp 64 °C. ^{1}H NMR ($CDCl_3$) δ 3.32 (dd, 1H, ^2J = 17.2 Hz, ^3J = 5.4 Hz, H-3), 3.87 (dd, 1H, ^2J = 17.2 Hz, ^3J = 8.6 Hz, H-3), 5.06 (dd, 1H, ^3J = 8.6 Hz, ^3J = 5.4 Hz, H-2), 6.91 (s, 1H, im H-4), 7.12 (s, 1H, im H-5), 7.49 (t, 1H, ^3J = 7.6 Hz, Ar H), 7.54 (d, 1H, ^3J = 7.6 Hz, Ar H), 7.70 (s, 1H, im H-2), 7.73 (t, 1H, ^3J = 7.6 Hz, Ar H), 7.84 (d, 1H, ^3J = 7.6 Hz, Ar H). IR (cm^{-1}): ν_{max} 3009, 1722, 1603, 1262.

2-(1*H*-Imidazol-1-yl)-3,4-dihydronaphthalen-1(2*H*)-one (13ii). Yield 65%, mp 71 °C.

2-(1*H*-Imidazol-1-yl)-6-methoxy-3,4-dihydronaphthalen-1(2*H*)-one (14ii). Yield 50%, mp 106 °C.

General Procedure for Synthesis of Compounds 12i−14i. A solution of the ketone (2.00 mmol) in 5 mL of anhydrous methanol was stirred under nitrogen in an ice bath. $NaBH_4$ (4.00 mmol) was added portionwise. After being stirred for 1 h at room temperature, the mixture was poured into water and extracted with dichloromethane. The organic layer was dried ($MgSO_4$), filtered, and evaporated in vacuo. The resulting alcohol was used for further reaction without purification.

2-(1*H*-Imidazol-1-yl)indan-1-ol (12i). Yield 96%. IR (cm^{-1}): ν_{max} 3541, 3032, 1660, 1504, 1276, 1084.

2-(1*H*-Imidazol-1-yl)-1,2,3,4-tetrahydronaphthalen-1-ol (13i). Yield 91%.

2-**(1*H*-Imidazol-1-yl)-6-methoxy-1,2,3,4-tetrahydronaphthalen-1-ol (14i).** Yield 83%.

General Procedure for Synthesis of Compounds 12−14. A mixture of 3 mL of acetic acid, 0.2 mL of sulfuric acid, and the alcohol (0.50 mmol) was stirred at 100 °C for 4 h. The reaction was poured into ice water and basified with a 6% sodium hydroxide solution. After extractions with dichloromethane, the organic layer was dried ($MgSO_4$), filtered, and evaporated in vacuo.

1-(1*H*-Inden-2-yl)-1*H*-imidazole (12). Purification by CC (CH_2Cl_2/MeOH, 97:3); yield 70%, mp 64 °C. ^{1}H NMR ($CDCl_3$) δ 3.87 (s, 2H, H-3), 6.78 (s, 1H, H-1), 7.22−7.24 (m, 2H, im H-4, Ar H), 7.30−7.33 (m, 2H, im H-5, Ar H), 7.38 (d, 1H, ^3J = 7.6 Hz, Ar H), 7.45 (d, 1H, ^3J = 7.6 Hz, Ar H), 8.09 (s, 1H, im H-2). IR (cm^{-1}): ν_{max} 2940, 1707, 1616, 1498, 1264, 1238. MS *m*/*z* 183 (MH^+).

1-(3,4-Dihydronaphthalen-2-yl)-1*H*-imidazole (13). Purification by CC (CH_2Cl_2/MeOH, 98:2); yield 96%, mp 186 °C (HCl salt).

1-(6-Methoxy-3,4-dihydronaphthalen-2-yl)-1*H*-imidazole (14). Purification by CC (CH_2Cl_2/MeOH, 98:2); yield 54%, mp 106 °C (HCl salt).

Synthesis of (*E*)- and (*Z*)-3-Styrylpyridine (15 and 16) A mixture of benzyl alcohol **15ii** (0.50 g, 4.62 mmol) and triphenylphosphonium bromide (1.59 g, 4.62 mmol) in 40 mL of toluene was refluxed for 12 h under a nitrogen atmosphere. After cooling, the phosphonium salt **15i** was filtered off, washed with diethyl ether, and dried in air. A suspension of the phosphonium salt **15i** (0.76 g, 1.75 mmol), K_2CO_3 (2.42 g, 17.50 mmol), pyridine-3-carbaldehyde (0.19 g, 1.75 mmol) and a few milligrams of 18-crown-6 in 50 mL of anhydrous dichloromethane was refluxed for 12 h. After being washed with water, the organic layer was dried ($MgSO_4$), filtered, and evaporated in vacuo. The mixture of isomers was purified by column chromatography and eluted with hexane/ethyl acetate (1:1).

3-[(*E*)-2-Phenylvinyl]pyridine (15). Yield 38%, mp 81 °C. ^{1}H NMR ($CDCl_3$) δ 7.08 (d, 1H, ^3J = 16.4 Hz, CH-Ph), 7.20 (d, 1H, ^3J = 16.4 Hz, CH-pyr), 7.31 (tt, 1H, ^3J = 7.6 Hz, ^4J = 1.3 Hz, Ar H), 7.35−7.40 (m, 3H, pyr H-5, Ar H), 7.54 (d, 2H, ^3J = 8.8 Hz, Ar H), 7.91 (dt, 1H,^3J = 7.9 Hz, ^4J = 1.6 Hz, pyr H-4), 8.50 (dd, 1H, ^3J = 4.7 Hz, ^4J = 1.6 Hz, pyr H-6), 8.75 (d, 1H, ^4J = 1.9 Hz, pyr H-2). IR (cm^{-1}): ν_{max} 3022, 1566, 962. MS *m*/*z* 182 (MH^+), 167, 115, 77, 51. Anal. ($C_{13}H_{11}N$) C, H, N.

3-[(*Z*)-2-Phenylvinyl]pyridine (16). Yield 52%, mp 145 °C (HCl salt).

Biological Methods

1. Enzyme Preparations. CYP19 and CYP17 preparations were obtained by described methods: microsomes from human placenta for CYP19[26] and the 50000*g* sediment of *E. coli* expressing human CYP17.[28]

2. Enzyme Assays. The following enzyme assays were performed as previously described: CYP19[26] and CYP17.[28]

3. Fission Yeast Assay. Fission yeast expressing human CYP11B2 (*S. pombe* PE1) was incubated with [4-^{14}C]-11-deoxycorticosterone as substrate and inhibitor at a concentration of 500 nM.[11] The enzyme reactions were stopped by addition of ethyl acetate. The conversion of the substrate was analyzed by HPTLC and a phosphoimaging system as described.[12,18]

4. Activity and Selectivity Assay with V79 Cells. V79 MZh 11B1 and V79 MZh 11B2 cells[24] were incubated with [4-^{14}C]-11-deoxycorticosterone as substrate and inhibitor on at least three different concentrations. The enzyme reactions were stopped by addition of ethyl acetate. After vigorous shaking and a centrifugation

step (10000*g*, 2 min), the steroids were extracted into the organic phase, which was then separated. The conversion of the substrate was analyzed by HPTLC and a phosphoimaging system as described.[12,18]

5. Inhibition of Human Hepatic CYPs. Compound **3** was tested for inhibition of human hepatic CYP3A4 and CYP2D6 at concentrations corresponding to the IC_{50} values of the well-known inhibitors ketoconazole and quinidine, respectively. The recombinantly expressed enzymes from baculovirus-infected insect microsomes (Supersomes) were used and the manufacturer's instructions were followed (www.gentest.com).

6. Modeling and Docking. By use of the recently resolved human cytochrome CYP2C9 structure (PDB code1OG5)[37] as template, a homology model was build and refined for CYP11B2 as described in refs 16−18. In this study selected compounds were docked into the refined homology model by use of FlexX-Pharm.[38] Pharmacophore constraints were applied to ensure the right binding mode of the inhibitors with the heme cofactor. For this purpose the standard Fe−N interaction parameters of FlexX[39,40] were modified and a directed heme−Fe−N interaction was defined perpendicular to the heme plane. The constraint requires the existence of an inhibitor-nitrogen-atom on the surface of an interaction cone with a 20° radius, which has its origin at the Fe atom and points perpendicular to the heme plane (with a length of 2.2 Å). Only docking solutions were accepted, which fulfill this constraint. For all other ligand−protein interactions, the standard FlexX interaction parameters and geometries were used.[39,40] The protein−ligand interactions were analyzed with the FlexX software.[39,40] The docked protein−inhibitor complex structures were used as a starting point for the subsequent molecular dynamics simulations, which were performed by applying the GROMOS96 force field[41] and the GROMACS program.[42] For the heme group the GROMOS96 force field parameters were used as provided with the GROMACS program package. A cutoff of 14 Å was used for the nonbonded interactions, and a time step of 1 fs was applied. The temperature was maintained by weak coupling to an external bath with a temperature coupling relaxation time of 0.1 ps.[43] Throughout the simulations, the bond lengths were constrained to ideal values by use of the LINCS procedure. No explicit solvent was included, because of the mainly hydrophobic character of the binding pocket. Potential solvent molecules were approximated through a dielectric constant of 4.0. Harmonic restraints were applied to all backbone atoms outside the binding pocket (all residues except residues 106−133, 212−221, 244−262, 305−332, 372−384, and 483−494). The systems were heated from 0 to 300 K over 200 ps and afterward 800 ps of molecular dynamics were performed at 300 K.

Regarding the superposition of Figure 3, the compounds were first generated in Hyperchem and the geometry was optimized in the steepest descent mode. Subsequently, all molecules were transferred to DS Viewer Pro. These compounds were aligned by use of three fixed atoms: the nitrogen of the heterocycle and the two adjacent carbons.

7. Caco-2 Transport Experiments. Caco-2 cell culture and transport experiments were performed according to Yee[29] with small modifications. Cell culture time was reduced to 10 days by increasing seeding density from 6.3×10^4 to 1.65×10^5 cells/cm^2. Four reference compounds, atenolol, ketoprofene, testosterone, and erythromycin, were used in each assay for validation of the transport properties of the Caco-2 cells. The compounds were applied to the cells as mixtures (cassette dosing) to increase the throughput of the cell permeability tests. The starting concentration of the compounds in the donor compartment was 50 μM in buffer containing either 1% ethanol or dimethyl sulfoxide (DMSO). After a preincubation step of 20 min at 37 °C, the reaction was started. The 12-well Transwellplates (Corning Costar) were stirred (20 rpm) at 37 °C. Samples were taken from the acceptor side after 60, 120, and 180 min and from the donor side after 0 and 180 min. Each experiment was run in triplicate. Monolayer integrity was checked by measuring the transepithelial electrical resistance (TEER) before the transport experiments and by measuring lucifer yellow cell permeability after each assay. All samples were analyzed by LC-MS/MS after 1:1 dilution with buffer of the opposite transwell chamber containing 2% acetic acid. The apparent cell permeability coefficients (P_{app}) were calculated from the equation $P_{app} = (dQ/dt)/Ac_0$, where dQ/dt is the mass appearance rate in the acceptor compartment, A is the surface area of the transwell membrane, and c_0 is the initial concentration in the donor compartment.

8. Metabolic Stability Assay. The assay was performed with rat microsomes (male pool, Gentest, Woburn, MA). The incubation solution contained a microsomal suspension of 0.15 mg of protein/mL in 0.1 M phosphate buffer, pH 7.4, and a NADPH-regenerating system (NADP 1 mM, glucose-6-phosphate 5 mM, glucose-6-phosphate dehydrogenase 5 units/mL, $MgCl_2$ 5 mM). After preincubation at 37 °C, the reaction was initiated by the addition of the test compound (a stock solution of 10 mM in 100% DMSO, diluted in 0.1 mM phosphate buffer, pH 7.4, to reach the final concentration of 5 μM with 2% final DMSO concentration). After 0, 30, 60, 120, and 180 min, 200 μL from the incubation was removed and added to ethyl acetate, containing the internal standard methoxyverapamil (5 μM), to stop the reaction. Subsequently, the samples were vortexed for 5 min and the organic layer was evaporated in a vacuum centrifuge, reconstituted in mobile phase, and analyzed by LC-MS/MS. The percentage of the remaining test compound was plotted against the corresponding time points, and the half-life time was calculated by using a standard fit of the data.

9. Metabolite Detection. The metabolites were identified by comparison of the total ion chromatograms between the incubation of time point zero and after 180 min. Once quasi-molecular ions were detected, they were subjected to further MS/MS analysis. The product ion MS/MS spectra of the parent compound were subsequently compared with the corresponding fragmentation pattern of putative metabolite structures. The specific fragment ion that showed a shift in its *m*/*z* was used for metabolite identification.

Acknowledgment. We thank the Deutsche Forschungsgemeinschaft (Ha 1513/6), the Saarland Ministry of Education, Culture and Science (ETTT Project), and the Fonds der Chemischen Industrie for financial support. C.S. is grateful to the European Postgraduate School 532 (DFG) for a scholarship. We thank Ms. Martina Palzer and Ms. Anja Palusczak for their help in performing the in vitro tests. Thanks are due to Professor Rita Bernhardt, Saarland University, and Organon NV, Oss, The Netherlands, for supplying us with the V79 cells.

Supporting Information Available: Elemental analysis results of compounds **1**−**17** and spectroscopic data of synthesized compounds **2**, **4**, **5**, **7**−**11**, **13**, **14**, **16**, **2i**, **4i**, **5i**, **7i**−**10i**, **13i**, **14i**, **3ii**−**6ii**, **8ii**−**10ii**, **14ii**, **4iii**−**6iii**, **8iii**, **10iii**, **12iii**, **6iv**, and **8iv**−**10iv**. This material is available free of charge via the Internet at http://pubs.acs.org.

References

(1) Kawamoto, T.; Mitsuuchi, Y.; Toda, K., Yokoyama, Y.; Miyakara, K.; Miura, S.; Onishi, T.; Ichihawa, Y.; Nakao, K.; Imura, H.; Ulick, S.; Shizuta, Y. Role of steroid 11β-hydroxylase and steroid 18-hydroxylase in the biosynthesis of glucocorticoids and mineralocorticoids in humans. *Proc. Natl. Acad. Sci. U.S.A.* **1992**, *89*, 1458−1462.

(2) Gomez-Sanchez, C. E.; Zhou, M. Y.; Cozza, E. N.; Morita, H.; Foecking, M. F.; Gomez-Sanchez, E. P. Aldosterone biosynthesis in the rat brain. *Endocrinology* **1997**, *138*, 3369−3373.

(3) Hatakeyama, H.; Miyamori, I.; Fujita, T.; Takeda, Y.; Takeda, R.; Yamamoto, H. Vascular aldosterone. *J. Biol. Chem.* **1994**, *269*, 24316−24320.

(4) White, P. C. Aldosterone: Direct effects on and production by the heart. *J. Clin. Endocrinol. Metab.* **2003**, *88*, 2376−2383.

(5) Satoh, M.; Nakamura, M.; Saitoh, H.; Satoh, H.; Akatsu, T.; Iwasaka, J.; Masuda, T.; Hiramori, K. Aldosterone synthase (CYP11B2) expression and myocardial fibrosis in the failing human heart. *Clin. Sci.* **2002**, *102*, 381−386.

(6) Sylvestre, J.-S.; Robert, V.; Heymes, C.; Aupetit-Faisant, B.; Mouas, C.; Moalic, J.-M.; Swynghedauw, B.; Delcayre, C. Myocardial production of aldosterone and corticosterone in the rat. *J. Biol. Chem.* **1998**, *273*, 4883−4891.

(7) Pitt, B.; Zannad, F.; Remme, W. J.; Cody, R.; Castaigne, A.; Perez, A., Palensky, J.; Wittes, J. The effect of spironolactone on morbidity and mortality in patients with severe heart failure. *N. Engl. J. Med.* **1999**, *341*, 709−717.

(8) Pitt, B.; Remme, W. J.; Zannad, F.; Neaton, J.; Martinez, F.; Roniker, B.; Bittman, R.; Hurley, S.; Kleiman, J.; Gatlin, M. Eplerenone, a selective aldosterone blocker, in patients with left ventricular dysfunction after myocardial infarction. *N. Engl. J. Med.* **2003**, *348*, 1309−21.

(9) Khan, N. U. A.; Movahed, A. The role of aldosterone and aldosterone-receptor antagonists in heart failure. *Rev. Cardiovasc. Med.* **2004**, *5*, 71−81.

(10) Juurlink, D. N.; Mamdani, M. M.; Lee, D. S.; Kopp, A.; Austin, P. C.; Laupacis, A.; Redelmeier, D. A. Rates of hyperkalemia after publication of the Randomized Aldactone Evaluation Study. *N. Engl. J. Med.* **2004**, *351*, 543−551.

(11) Hartmann, R. W. Selective inhibition of steroidogenic P450 enzymes: current status and future perspectives. *Eur. J. Pharm. Sci.* **1994**, *2*, 15−16.

(12) Ehmer, P. B.; Bureik, M.; Bernhardt, R.; Müller, U.; Hartmann, R. W. Development of a test system for inhibitors of human aldosterone synthase (CYP11B2): Screening in fission yeast and evaluation of selectivity in V79 cells. *J. Steroid Biochem. Mol. Biol.* **2002**, *81*, 173−179.

(13) Hartmann, R. W.; Müller, U.; Ehmer, P. B. Discovery of selective CYP11B2 (aldosterone synthase) inhibitors for the therapy of congestive heart failure and myocardial fibrosis. *Eur. J. Med. Chem.* **2003**, *38*, 363−366.

(14) Taymans, S. E.; Pack, S.; Pak, E.; Torpy, D. J.; Zhuang, Z.; Stratakis, C. A. Human CYP11B2 (aldosterone synthase) maps to chromosome 8q24.3. *J. Clin. Endocrinol. Metab.* **1998**, *83*, 1033−1036.

(15) Voets, M.; Müller-Vieira, U.; Marchais-Oberwinkler, S.; Hartmann, R. W. Synthesis of amidinohydrazones and evaluation of their inhibitory effect towards aldosterone synthase (CYP11B2) and the formation of selected steroids. *Arch. Pharm. Pharm. Med. Chem.* **2004**, *337*, 411−416.

(16) Ulmschneider, S.; Müller-Vieira, U.; Mitrenga, M.; Hartmann, R. W.; Oberwinkler-Marchais, S.; Klein, C. D.; Bureik, M.; Bernhardt, R.; Antes, I.; Lengauer, T. Synthesis and evaluation of imidazolylmethylene-tetrahydronaphthalenes and imidazolylmethylene-indanes: Potent inhibitors of aldosterone synthase. *J. Med. Chem.* **2005**, *48*, 1796−1805.

(17) Ulmschneider, S.; Müller-Vieira, U.; Klein, C. D.; Antes, I.; Lengauer, T.; Hartmann, R. W. Synthesis and evaluation of (pyridylmethylene)-tetrahydronaphthalenes/-indanes and structurally modified derivatives: Potent and selective inhibitors of aldosterone synthase. *J. Med. Chem.* **2005**, *48*, 1563−1575.

(18) Voets, M.; Antes, I.; Scherer, C.; Müller-Vieira, U.; Biemel, K.; Barassin, C.; Oberwinkler-Marchais, S.; Hartmann, R. W. Heteroaryl substituted naphthalenes and structurally modified derivatives: Selective inhibitors of CYP11B2 for the treatment of congestive heart failure and myocardial fibrosis. *J. Med. Chem.* **2005**, *48*. 6632−6642.

(19) Miyaura, N.; Suzuki, N. Palladium-catalyzed cross-coupling reactions of organoboron compounds. *Chem. Rev.* **1995**, *95*, 2457−2483.

(20) Bencze, W. L.; Barsky, L. I. Selective adrenal cortical and gonadal inhibitors. *J. Med. Pharm. Chem.* **1962**, *5*, 1298−1306.

(21) Cozzi, P.; Branzoli, U.; Ferti, C.; Pillan, A.; Severino, D.; Tonani, R. *N*-Imidazolyl derivatives of the naphthalene and chroman rings as thromboxane A_2 synthase inhibitors. *Eur. J. Med. Chem.* **1991**, *26*, 423−433.

(22) Häusler, A.; Monnet, G.; Borer, C.; Bhatnagar, A. S. Evidence that corticosterone is not an obligatory intermediate in aldosterone biosynthesis in the rat adrenal. *J. Steroid Biochem.* **1989**, *34*, 567−570.

(23) Demers, L. M.; Melby, J. C.; Wilson, T. E.; Lipton, A.; Harvey, H. A.; Santen, R. J. The effects of CGS 16949A, an aromatase inhibitor, on adrenal mineralocorticoid biosynthesis. *J. Clin. Endocrinol. Metab.* **1990**, *70*, 1162−1166.

(24) Denner, K.; Doehmer, J.; Bernhardt, R. Cloning of CYP11B1 and CYP11B2 from normal human adrenal and their functional expression in COS-7 and V79 chinese hamster cells. *Endocr. Res.* **1995**, *21*, 443−448.

(25) Thompson, E. A.; Siiteri, P. K. Utilization of oxygen and reduced nicotinamide adenine dinucleotide phosphate by human placental microsomes during aromatization of androstenedione. *J. Biol. Chem.* **1974**, *249*, 5364−5372.

(26) Hartmann, R. W.; Batzl, C. Aromatase inhibitors. Synthesis and evaluation of mammary tumor inhibiting activity of 3-alkylated 3-(4-aminophenyl)piperidine-2,6-diones. *J. Med. Chem.* **1986**, *29*, 1362−1369.

(27) Ehmer, P. B.; Jose, J.; Hartmann, R. W. Development of a simple and rapid assay for the evaluation of inhibitors of human 17α-hydroxylase-$C_{17,20}$-lyase (P450c17) by coexpression of P450c17 with NADPH-cytochrome-P450-reductase in *Escherichia coli*. *J. Steroid Biochem. Mol. Biol.* **2000**, *75*, 57−63.

(28) Hutschenreuter, T. U.; Ehmer, P. B.; Hartmann, R. W. Synthesis of hydroxy derivatives of highly potent nonsteroidal CYP17 inhibitors as potential metabolites and evaluation of their activity by a non cellular assay using recombinant enzyme. *J. Enzyme Inhib. Med. Chem.* **2004**, *19*, 17−32.

(29) Yee, S. In vitro permeability across Caco-2 cells (colonic) can predict in vivo (small intestinal) absorption in men—fact or myth. *Pharm. Res.* **1997**, *14*, 763−766.

(30) Tannergren, C.; Langguth, P.; Hoffmann, K. J. Compound mixtures in Caco-2 cell permeability screens as a means to increase screening capacity. *Pharmazie* **2001**, *56*, 337−342.

(31) Laitinen, L.; Kangas, H.; Kaukonen, A. M.; Hakala, K.; Kotiaho, R.; Kostiainen, R.; Hirvonen, J. N-in-one permeability studies of heterogeneous sets of compounds across Caco-2 cell monolayers. *Pharm. Res.* **2003**, *20*, 187−197.

(32) Saito, H.; Fukasawa, Y.; Otsubo, Y.; Yamada, K.; Sezaki, H.; Yamashita, S. Carrier-mediated transport of macrolide antimicrobial agents across Caco-2 cell monolayers. *Pharm. Res.* **2000**, *17*, 761−765.

(33) Fiebeler, A.; Nussberger, J.; Shagdarsuren, E.; Rong, S.; Hilfenhaus, G.; Al-Saadi, N.; Dechend, R.; Wellner, M.; Meiners, S.; Maser-Gluth, C.; Jeng, A. Y.; Webb, R. L.; Luft, F. C.; Muller, D. N. Aldosterone synthase inhibitor ameliorates angiotensin II-induced organ damage. *Circulation* **2005**, *111*, 3087−3094.

(34) Lindley, W. A.; MacDowell, D. W. H. Keto−enol tautomerism in the thiophene analogues of naphthacen-5-one. *J. Org. Chem.* **1982**, *47*, 705−709.

(35) Hauser, C. R.; Skell, P. S.; Bright, R. D.; Renfrow, W. B. Removal of hydrogen bromide from certain β-phenylalkyl bromides by means of potassium amide in liquid ammonia. *J. Am. Chem. Soc.* **1947**, *69*, 589−593.

(36) Li, W.; Nelson, D. P.; Jensen, M. S.; Hoerrner, R. S.; Cai, D.; Larsen, R. D.; Reider, P. J. An improved protocol for the preparation of 3-pyridyl- and some arylboronic acids. *J. Org. Chem.* **2002**, *67*, 5394−5397.

(37) Williams, P. A.; Cosme, J.; Ward, A.; Angove, H. C.; Matak Vinkovic, D.; Jhoti, H. Crystal structure of human cytochrome P4502C9 with bound warfarin. *Nature* **2003**, *424*, 464−468.

(38) Hindle, S. A.; Rarey, M.; Buning, C.; Lengauer, T. Flexible docking under pharmacophore type constraints. *J. Comput.-Aided Mol. Des.* **2002**, *16*, 129−149.

(39) Rarey, M.; Kramer, B.; Lengauer, T.; Klebe G. A fast flexible docking method using an incremental construction algorithm. *J. Mol. Biol.* **1996**, *261*, 470−489.

(40) Rarey, M.; Kramer, B.; Lengauer, T. Multiple automatic base selection: Protein−ligand docking based on incremental construction without manual intervention. *J. Comput.-Aided Mol. Des.* **1997**, *11*, 369−384.

(41) Scott, W. R. P.; Hünenberger, P. H.; Tironi, I. G.; Mark, A. E.; Billeter, S. R.; Fennen, J.; Torda, A. E.; Huber, T.; Krüger, P.; van Gunsteren, W. F. The GROMOS Biomolecular Simulation Program Package. *J. Phys. Chem. A* **1999**, *103*, 3596−3607.

(42) Lindahl, E.; Hess, B.; van der Spoel, D. GROMACS 3.0: a package for molecular simulation and trajectory analysis. *J. Mol. Mod.* **2001**, *7*, 306−317.

(43) Berendsen, H. J. C.; Postma, J. P. M.; van Gunsteren, W. F.; Hermans, J. Interaction models for water in relation to protein hydration. In *Intermolecular Forces*; Pullman, B., Ed.; Reidel Publishing Co.: Dordrecht, The Netherlands, 1981; pp 331−342.

JM060055X